
Lo-Hi: Practical ML Drug Discovery Benchmark

Simon Steshin

Independent Researcher

simon.steshin@gmail.com

Abstract

Finding new drugs is getting harder and harder. One of the hopes of drug discovery is to use machine learning models to predict molecular properties. That is why models for molecular property prediction are being developed and tested on benchmarks such as MoleculeNet. However, existing benchmarks are unrealistic and are too different from applying the models in practice. We have created a new practical *Lo-Hi* benchmark consisting of two tasks: Lead Optimization (Lo) and Hit Identification (Hi), corresponding to the real drug discovery process. For the Hi task, we designed a novel molecular splitting algorithm that solves the Balanced Vertex Minimum k -Cut problem. We tested state-of-the-art and classic ML models, revealing which works better under practical settings. We analyzed modern benchmarks and showed that they are unrealistic and overoptimistic.

Review: <https://openreview.net/forum?id=H2Yb28qGLV>

Lo-Hi benchmark: https://github.com/SteshinSS/lohi_neurips2023

Lo-Hi splitter library: https://github.com/SteshinSS/lohi_splitter

1 Introduction

Drug discovery is the process of identifying molecules with therapeutic properties [1]. To serve as a drug, a molecule must possess multiple properties simultaneously [2]. It must be stable [3], yet easily eliminated from the body [4], able to reach its target [5, 6, 7], non-toxic [8], cause minimal side effects [9], and therapeutically active on the target [10, 11].

To identify such molecules, researchers develop Molecular Property Prediction (MPP) models. These models are used in a virtual screening, during which the models are used to make predictions for a large number of molecules, after which the molecules with the best estimated property are selected for experimental validation [12, 13, 14, 15, 16].

To enable comparisons between various architectures, the research community relies on standardized benchmarks to evaluate model performance [17, 18, 19, 20, 21, 22, 23]. The prevailing assumption is that models with superior metrics on these benchmarks are more suitable for real-world applications.

We believe this assumption is false. Modern benchmarks test in non-realistic conditions on impractical tasks. In this paper, we introduce two new practical drug discovery ML tasks — Hit Identification and Lead Optimization — that are often encountered in most drug discovery campaigns. We demonstrate that none of the benchmarks assess models for these tasks, which is why we propose seven new practical datasets that better imitate real-life drug discovery scenarios. To prepare Hi datasets, we designed a novel molecular splitter algorithm that solves Balanced Vertex Minimum k -Cut problem using Integer Linear Programming with heuristics.

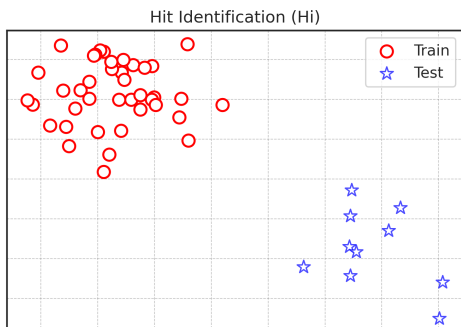


Figure 1: Hit Identification (Hi) task

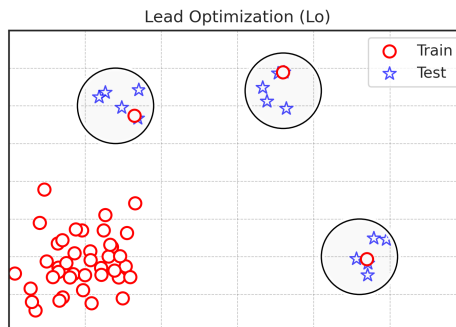


Figure 2: Lead Optimization (Lo) task

2 Practical drug discovery

2.1 Hit Identification (Hi)

Drug discovery involves multiple stages. When the potential mechanism of action is known, an early step is Hit Identification. During this phase, chemists search for a "hit" - a molecule with the potential to become a drug [24]. A viable hit must exhibit some level of activity towards the target (e.g., K_i less than $10\text{ }\mu\text{M}$) and possess novelty, meaning it is eligible for patent protection.

Clinical trials can incur costs in the hundreds of millions of dollars [25, 26], making it risky to pursue non-patentable molecules. Consequently, companies prioritize patentable molecules from the outset. Novelty is an essential aspect of this process. In practice, medicinal chemists often pre-filter their chemical libraries before the virtual screening, eliminating molecules that exhibit a Tanimoto similarity above a specific threshold to molecules with known activity [10, 11, 16, 27, 28, 29].

2.2 Lead Optimization (Lo)

Following Hit Identification, the next stage is Lead Optimization. Once a novel, patentable molecule with activity towards the desired target is identified, its closest analogs are also likely to exhibit activity [30]. In this phase, medicinal chemists often make minor modifications to the hit molecule to enhance its target activity, selectivity, and other properties [31, 32]. Unlike in Hit Identification, novelty usually is not a priority during Lead Optimization. Instead, the objective is to discover molecules that are similar to the original hit but possess improved characteristics.

This is related to the field of goal-directed molecular generation [33], which is occasionally formulated as the problem of searching for molecules with maximal activity within the ϵ -neighborhood of a known hit [34, 35], within some scaffold [36], or as an optimization process in the latent space [37]. These works use predictive ML models to distinguish between minor chemical modifications [38]. The effectiveness of these models in their ability to distinguish between molecules with small modifications remains unclear.

2.3 Model Selection

In this context, Lead Optimization (Lo) and Hit Identification (Hi) represent contrasting tasks. Hi ML models are expected to demonstrate their generalization capabilities by predicting properties of molecules significantly different from the training set. Conversely, Lo ML models should predict properties of minor modifications of molecules with known activity.

For selecting the appropriate ML model or adjusting its hyperparameters, it is crucial to test the model under conditions similar to its intended application. In Hi, models must identify novel molecules markedly different from known active ones, implying the models should be tested on molecules distinctly different from the training set. Conversely, Lo applies ML models to molecules resembling known active ones. The null Structure-Activity Relationship hypothesis assumes that

small modifications will not alter the molecule’s properties [30, 39]. Consequently, Lo ML models should be evaluated based on their ability to make predictions that surpass the null hypothesis.

We show that modern benchmarks mix these two scenarios, which is why it remains unclear how effectively models can generalize to truly novel molecules and how proficiently they can distinguish minor modifications, thereby guiding molecular optimization. Furthermore, we untangle these scenarios using a novel benchmark, demonstrating that **different architectures are better suited for different tasks**.

3 Novelty

But how to measure novelty? From a commercialization and regulatory perspective, a novel molecule is one that can be patented. Contemporary patents consist of human-written text and incorporate non-trivial substitutions, rendering the assessment of a molecule’s patentability a complex task for legal professionals. To date, this process has not been automated. Additionally, during the Hit Identification, not only must the hit be patentable — its neighborhood should be patentable as well to make Lead Optimization possible. When dealing with an extensive chemical library, these challenges make patentability an impractical criterion for determining novelty.

While chemists agree that minor substitutions likely do not alter a molecule’s function, a consensus on the distinction between a new molecule and a modified version of an existing one remains elusive. One might hope to find a general similarity threshold that would separate similar molecules with presumably the same activity from distinct molecules. This hope led to the "0.85 myth" [40], which proved to be false due to the significant variability of such thresholds across different targets [41]. About molecular similarity, it was said [42, 41], "Similarity is in the eye of the beholder." Nevertheless, a practical criterion exists.

In study [43] 143 experts from regulatory authorities (FDA, FDA of Taiwan, EMA, PMDA) were shown 100 molecular pairs and asked if the molecules should be regarded as structurally similar. This study is especially notable because it simulates a real-life scenario in which a regulatory committee (EMA’s Committee for Medicinal Products for Human Use) decides if a new drug is novel enough to grant it a beneficial status: orphan drug designation. The study shows that when two molecules have Tanimoto similarity ≈ 0.4 with ECFP4 fingerprints [44], half of the experts regard them as dissimilar, which is sufficient to conclude the novelty of the drug. See Appendix G for our reproduction.

While Tanimoto similarity with ECFP4 fingerprints has its own disadvantages such as size bias [45], its simplicity makes it possible to quickly measure the similarity of molecules, so there are practical [16] and theoretical [46, 47] works that use "Tanimoto similarity < 0.4 " as a novelty criterion. Because of the practical evaluation in real-life scenarios and efficiency, we assess novelty using Tanimoto similarity with ECFP4 fingerprints in our benchmark.

4 Our contribution

- We suggest two new practical drug discovery ML tasks — Hit Identification and Lead Optimization — that better imitate real-life scenarios;
- We designed a novel molecular splitting algorithm for the Hi task;
- We propose seven new practical datasets;
- We demonstrate that modern ML drug discovery benchmarks simulate impractical scenarios;
- We evaluate modern and classic ML algorithms on our benchmark.

5 Modern benchmarks test neither Lo nor Hi

To select a model or its hyperparameters, we must evaluate them under the conditions in which they will be used. We demonstrate that none of the modern benchmarks correspond to realistic conditions, thus raising questions about their suitability for evaluating practical machine learning models. Although it is impossible to examine every existing benchmark due to their sheer number, we have opted to assess a variety of benchmarks using different data, different preprocessing techniques, and originating from different authors. We will initially focus on standard benchmarks, while in

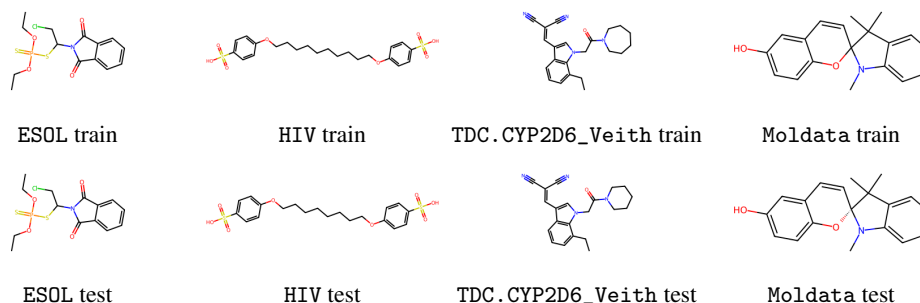


Figure 3: Common benchmarks contain highly similar molecules across different splits.

the section 6, we will explore more exotic and specialized ones. We provide additional analysis in Appendix D.

5.1 MoleculeNet: ESOL

MoleculeNet [17] is a widely-used benchmark for ML drug discovery, consisting of 17 datasets, including the ESOL dataset with water solubility data. This dataset is frequently used in studies for model comparisons [48, 49, 50, 51, 52, 53]. While the authors recommend a random train-test split, we discovered that it leads to 76% of the test molecules having a neighbor in the train with Tanimoto similarity > 0.4 , making ESOL unsuitable for Hi scenario (see Fig. 3). It is also unclear how well the dataset represents the Lo scenario, as the distinct 24% of the train contributes to the evaluation, and the RMSE metric can be significantly improved over the constant baseline, even without identifying minor chemical modifications.

5.2 MoleculeNet: HIV

In benchmarks, train and test sets are typically split using random, scaffold, or occasionally time splits when time stamps are available. It has been frequently observed that random splits can result in highly similar molecules in both train and test sets, leading to overly optimistic and impractical estimations. For example: "Random splitting, common in machine learning, is often not correct for chemical data" [17]. Thus, scaffold splitting [54] is sometimes suggested as an alternative.

Scaffold splitting [54] is a method where each molecule is represented by a graph consisting of ring systems, linkers and side chains. A group of molecules may correspond to a single graph, in which case they are assigned to the same partition.

The MoleculeNet HIV dataset (ubiquitous in evaluation [55, 56, 57, 58, 59]) recommends using scaffold splitting, as it is believed to better reflect the process of discovering new molecules: "As we are more interested in discovering new categories of HIV inhibitors, scaffold splitting [...] is recommended" [17]. Although scaffold splitting makes the train set more distinct from the test set, it is still insufficient for the scenario of finding novel molecules. We discovered that 56% of HIV test molecules have a train neighbor with a Tanimoto similarity > 0.4 , indicating the dataset is unsuitable for the Hi scenario (see Fig. 3). Additionally, the dataset is unsuitable for the Lo scenario due to its binary label, rather than a continuous value.

5.3 Therapeutic Data Commons: TDC.CYP2D6_Veith

The Therapeutic Data Commons [18] is a novel platform designed for evaluating machine learning models in drug discovery. We examined the largest dataset, TDC.CYP2D6_Veith, within the Single-Instance Learning Tasks category. Although a scaffold split is recommended, the dataset is deemed unsuitable for the Hi scenario, as 78% of test molecules possess a training neighbor exhibiting a Tanimoto similarity greater than 0.4 (see Fig. 3). Additionally, the dataset is unsuitable for the Lo scenario due to its binary label, rather than a continuous value.

5.4 MolData

MolData [19] is a recent benchmark for MPP based on PubChem data. The authors themselves analyzed the novelty of the molecules within the subset and found their scaffold split to be unrealistic: “[...] more than 44% of the molecules within the MolData dataset have at least one other similar molecule to them with a Tanimoto Coefficient of 0.7 or higher. This high percentage of the similarity can denote lack of diversity within this portion of the dataset.”

The authors use scaffold split to increase the difference between the train and the test, but we found that at least 88% of the molecules in the test have a similar molecule in the train with a Tanimoto similarity > 0.4 , making the dataset unsuitable for the Hi scenario (see Fig. 3). Additionally, the dataset is unsuitable for the Lo scenario due to its binary label, rather than a continuous value.

6 Related works

6.1 Out-of-distribution MPP

In the Hi scenario, the training and test sets are significantly different to simulate the search for new molecules, making the Hi scenario interpretable as an Out-Of-Distribution (OOD) task. Although OOD benchmarks already exist for machine learning-based drug discovery, they do not align with practical drug discovery applications.

DrugOOD [20] is a drug discovery benchmark dedicated to Out-Of-Distribution prediction. The authors accurately observe that "In the field of AI-aided drug discovery, the problem of distribution shift [...] is ubiquitous", and therefore suggest assay-based, scaffold-based, or molecular size-based partitions to create a distribution shift. However, their benchmark does not correspond to practical drug discovery, as it involves predicting average activity for all ChEMBL targets simultaneously in ligand-based drug discovery datasets. This approach is impractical because, in reality, researchers are not interested in average activity across ChEMBL targets, but rather in activity on a specific target.

G00D [21] is a benchmark explicitly designed to separate covariate and concept shifts. We examined the G00D-HIV dataset, as it is a MPP benchmark containing a significant amount of diverse data (see the #Circles in Appendix A). In all Out-Of-Distribution test partitions, more than 40% of molecules have a neighbor in the training set at a Tanimoto similarity more than 0.4, making the dataset unsuitable for the Hi scenario.

During the NeurIPS review period, Valence Labs and Laval University jointly published work — independent from ours — investigating Molecular-Out-Of-Distribution generalization [60]. Their research is akin to our Hi-scenario, but the authors studied different data splits, employed different models, and investigated uncertainty calibration.

6.2 Activity cliff

Activity cliff is a pair of structurally similar compounds that are active against the same bio-target but significantly different in binding potency [61, 22].

Recently, several remarkable studies have emerged, seeking to establish a standard benchmark for Activity Cliff Prediction [22, 23]. These works have inspired us to create our own benchmark. While Activity Cliff Prediction may be advantageous in the Lo scenario, it is inadequate for guiding molecule optimization. In the Lo scenario, it is essential not only to identify extreme activity cliffs with a 10x difference in activity but also to predict minor activity fluctuations. We propose alternative splits and metrics in the Lo scenario.

7 Results

7.1 Hi-splitter

To simulate the Hi scenario, it is necessary to divide the dataset into training and testing subsets such that any pair of molecules from different partitions has a ECFP4 Tanimoto similarity of less than 0.4. Despite the fact that the scaffold splitter produces a more diverse division than random splitter, we observe that it is inadequate for an effective Hi scenario.

A greedy approach is to implement the conventional scaffold split and discard from the test set any molecules excessively similar to those in the training set. The issue with this method, however, is that data points are costly, and it is desirable to minimize the number of discarded molecules. Consequently, we have developed a novel algorithm for strict dataset splitting, which discards fewer molecules than the greedy algorithm.

Let us consider molecules $X = \{x_1, \dots, x_n\}$. We construct a neighborhood graph $G = (V, E)$, where each molecule x_i corresponds to a vertex $v_i \in V$. Two vertices are connected by an edge if and only if the associated molecules have a similarity to each other greater than threshold t : $e_{vu} \in E \Leftrightarrow T(x_v, x_u) > t$, where T is Tanimoto Similarity with ECFP4 fingerprints. In such a graph, connected components can be assigned to the training or testing sets independently. However, in practice, 95% of the molecules belong to a single connectivity component. Our goal is to remove the minimum number of vertices such that the giant component breaks up into multiple components with size constraints, thereby enabling us to distribute them between the training and testing sets.

This problem is known as the Balanced Vertex Minimum k -Cut and has been extensively researched in literature [62, 63, 64]. A review of similar problems can be found elsewhere [65, 66]. Similar to [62] we formulate the Integer Linear Programming formulation.

Let K denote the set of integers $\{1, 2, \dots, k\}$. Let $G = (V, E)$ represent a simple connected graph that we are going to split:

$$V = \cup_{i=1}^k V_i \cup V_0 \quad \forall i \neq j \quad V_i \cap V_j = \emptyset$$

For all vertices $v \in V$ and for all integers $i \in K$, let us associate a binary indicator y_v^i such that:

$$y_v^i = \begin{cases} 1, & \text{if } v \in V_i \\ 0, & \text{otherwise} \end{cases}$$

Note that V_0 denotes the set of removed vertices, so if $\sum_{i \in K} y_v^i = 0$ then the vertex v is in V_0 .

Let $b_i \in \mathbb{N}$ be a lower bound on the cardinality $|V_i|$ of partition V_i . We need it to get partitions with size constraints, e.g. 80% in train and 20% in test. Let w_v be the weights of the nodes. In simple formulation we take $w_v = 1$. We formulate the Balanced Vertex Minimum k -Cut as follows:

$$\max \sum_{i \in K} \sum_{v \in V} w_v y_v^i \quad (1)$$

$$\sum_{i \in K} y_v^i \leq 1 \quad \forall v \in V \quad (2)$$

$$y_u^i + y_v^j \leq 1 \quad \forall i \neq j \in K, \forall e_{uv} \in E \quad (3)$$

$$\sum_{v \in V} y_v^i \geq b_i \quad \forall i \in K \quad (4)$$

$$y_v^i \in \{0, 1\} \quad \forall i \in K, \forall v \in V \quad (5)$$

Equation (1) minimizes the weight of removed molecules V_0 . Equation (2) states that each vertex v should be in one partition maximum. Equation (3) ensures there is no connectivity between different partitions, so for each edge $e_{uv} \in E$ if u is in V_i partition, then the other vertex v is either in V_i as well, or in V_0 , meaning it was removed. Equation (4) puts constraints on the size of the partitions V_i .

While this formulation was effective on small-scale graphs (around 100 vertices), we found it too slow for a real DRD2 activity dataset with 6k molecules. To our knowledge, existing literature [62, 65, 67, 68] typically involves small graphs from the standard benchmarks with a maximum node count of several hundred. To expedite computation, we implemented a graph coarsening approach. The basic idea is outlined here, while the formal algorithm is detailed in Appendix E.

We initially performed Butina clustering [69] on molecules and created a coarse graph wherein the vertices correspond not to individual molecules but to clusters of molecules. In the coarsened graph,

each vertex is assigned a weight w_v equal to the number of molecules in the respective cluster. This approach accelerated computations and enabled us to partition the HIV dataset consisting of 40k molecules, removing fewer vertices than would be the case with the greedy approach (See Table 1).

Table 1: Number of removed molecules for 0.9:0.1 split

Method	DRD2	HIV
Greedy	1066 (17.0%)	5851 (14.2%)
Hi-Splitter	97 (1.5%)	1598 (3.8%)

7.2 Lo-Hi benchmark

We conducted an analysis of numerous drug discovery benchmarks, yet none seemed to align with the actual drug discovery process. Consequently, we prepared seven datasets and are now making them available to the community.

We selected datasets that represent realistic drug discovery problems, contain substantial amounts of qualitative data, and cover a diverse chemical space. Diversity was assessed using the recently introduced #Circles metric [70]. As the source code was unavailable at the time of writing, we employed our own implementation of the greedy algorithm outlined in [70]: Appendix H. We provide additional statistics for the original datasets in the Appendix A.

We propose three distinct train-test splits for each dataset. We advise adjusting hyperparameters solely on the first split, applying the same hyperparameters to train and assess models on splits #2 and #3, and comparing models by averaging metrics across the splits. Datasets are released under the MIT license.

7.2.1 Hi

In the Hit Identification scenario, we aim to predict binary labels for new molecules that significantly differ from those in the training set. We prepared four datasets which we divided into training and testing sets, ensuring that the Tanimoto similarity between any molecule in the test set and those in the training set is less than 0.4. See Fig. 1. Additionally, we show that such a split predicts experimental outcomes better than the scaffold split (Appendix F).

DRD2-Hi involves predicting dopamine receptor inhibition, a GPCR target of therapeutic importance in schizophrenia [71, 72] and Parkinson’s disease [73, 74]. To create this dataset, we obtained Ki data for DRD2 from ChEMBL30 [75], cleaned it (see Appendix A), and binarized it so that molecules with $K_i < 10\mu\text{M}$ are considered active.

HIV-Hi is an HIV dataset from the Drug Therapeutics Program AIDS Antiviral Screen that measures the inhibition of HIV replication. We obtained the prepared dataset from MoleculeNet [17].

DRD2-Hi and HIV-Hi are large. However, real-life data often comes in limited quantities. To simulate this crucial scenario, we prepared a smaller challenging dataset, KDR-Hi. This dataset is based on the ChEMBL30 IC50 data associated with vascular endothelial growth factor receptor 2, a kinase target for cancer treatment [76]. Its creation process was similar to that of DRD2-Hi, but we restricted the training folds to just 500 molecules.

The Sol-Hi dataset draws from a public solubility dataset at Biogen [77]. We binarized this data such that molecules with a solubility of less than $10\mu\text{g/mL}$ were assigned a positive label.

Each dataset was divided into distinct training and testing sets. We used the Hi-splitter with $k = 3$ to obtain three highly dissimilar subsets: $\{F_1, F_2, F_3\}$. These subsets were then combined to create three distinct folds, each with a unique test set. For instance, for the first fold, the training set was $train_1 = \{F_1, F_2\}$ and the test set was $test_1 = \{F_3\}$. This methodology enabled us to assess the variability in quality resulting from using different data with the same models.¹

Hi Metric For our benchmark, we have selected the PR AUC. As a simple binary classification metric without parameters, it is implemented in most libraries and normalized to a range of [0, 1].

¹The DRD2-Hi preparation code can be found at `notebooks/data/03_split_drd2_hi.ipynb`.

The PR AUC favors early recognition models [78] and does not appeal to wrong intuition among readers in an unbalanced setting.

7.2.2 Lo

In the Lead Optimization scenario, we aim to predict the activity of molecules that are highly similar to those in the training set. As similar molecules tend to exhibit similar activity, our focus is not on predicting binary labels, but rather on ranking, which indicates whether a modification increases the activity or not.

To simulate the Lead Optimization scenario, we isolated clusters of molecules with intracluster similarity ≥ 0.4 and consisting of ≥ 5 molecules. We included them in the test dataset. In practical Lead Optimization, the activity of a given hit is already known; thus, for each cluster, we retained exactly one molecule with a similarity ≥ 0.4 to that cluster in the training set. See Fig. 2. We provide additional analysis in Appendix A.

In order to confirm the validity of the Lo benchmark, we ensured that the intracluster variation in activity exceeds the experimental noise (See Appendix B). This step is critical, as if the variance within a cluster of similar molecules is not significantly greater than the experimental noise, it would not make sense to test models on such molecules — under these conditions, even an ideal model would struggle to make accurate predictions. The formal pseudocode can be found in Appendix C.

We assembled three datasets: DRD2-Lo, KCNH2-Lo and KDR-Lo. Both DRD2-Lo and KDR-Lo are based on the same data as their respective Hi counterparts but feature a different split between training and testing sets. KCNH2 is an ion channel that regulates heartbeat, and its inhibition can cause dangerous side effects [79]. Consequently, bioassays for KCNH2 are used as a screening method for cardiotoxicity. We extracted IC50 data from ChEMBL30, cleaned it, and divided it into training and testing sets.

Each dataset was split three times using different random seeds, resulting in three folds. This method enables us to assess the variability in quality when using different data with the same models.²

Lo Metric Our goal is to determine whether the models can make better predictions than assuming "the modified molecule active in the same manner as the original hit." We chose Spearman’s correlation coefficient as our metric, calculated within each cluster and averaged across clusters. This metric does not rely on intracluster variation, depends solely on the ranking of molecules within the cluster, and is normalized, between minus one (ideally wrong), zero (random) and one (ideal), rendering it easily interpretable.

7.3 Evaluation

We evaluated both traditional and state-of-the-art ML models on our benchmark. We meticulously executed the hyperparameter search, following the procedure outlined in Appendix H. Results are presented in Table 2. The best scores for fingerprint and graph models are highlighted in bold. It should be noted that the mean and standard deviation were calculated not for random seeds, but within different folds.

We found that the best models varied for the Hi and Lo tasks. The most effective model for the Hi task was the Chemprop graph neural network [80], aligning with its real-world success [16, 28, 29]. The second-best were gradient boosting and KNN for the small KDR-Hi dataset.

Conversely, for the Lo task, the SVM model was found to be the most proficient, which corroborates previous works on activity cliffs [23]. Only for the small KDR-Lo did Chemprop outperform SVM, but even then, the performance was not satisfactory. We further provide a per-cluster Spearman distribution for SVM in Appendix I. The limited inability of Chemprop to distinguish minor modifications may be due to the limited expressivity of graph neural networks. However, this was surprising to us, considering the limited expressivity of binary fingerprints as well.

²The DRD2-Lo preparation code can be found at `notebooks/data/04_split_drd2_lo.ipynb`.

Table 2: *Lo-Hi* results. PR AUC for Hi and mean Spearman for Lo.

Model	DRD2-Hi	HIV-Hi	KDR-Hi	So1-Hi	DRD2-Lo	KCNH2-Lo	KDR-Lo
Dummy baseline	0.677±0.061	0.04±0.014	0.609±0.081	0.215±0.008	0.000±0.0	0.000±0.0	0.000±0.0
KNN (Tanimoto distance, ECFP4)	0.706±0.047	0.067±0.029	0.646±0.048	0.426±0.022	0.195±0.053	0.164±0.014	0.130±0.034
KNN (Tanimoto distance, MACCS)	0.702±0.042	0.072±0.036	0.610±0.072	0.422±0.009	0.211±0.041	0.036±0.022	0.071±0.02
Gradient Boosting (ECFP4)	0.736±0.05	0.08±0.038	0.607±0.067	0.429±0.006	0.145±0.052	0.37±0.003	0.076±0.036
Gradient Boosting (MACCS)	0.751±0.063	0.058±0.03	0.603±0.074	0.502±0.045	0.197±0.043	0.216±0.032	0.100±0.026
SVM (ECFP4)	0.677±0.061	0.04±0.014	0.611±0.081	0.298±0.047	0.311±0.015	0.472±0.014	0.158±0.051
SVM (MACCS)	0.713±0.05	0.042±0.015	0.605±0.082	0.308±0.021	0.219±0.02	0.133±0.024	0.074±0.034
MLP (ECFP4)	0.717±0.063	0.049±0.019	0.626±0.047	0.403±0.017	0.094±0.059	0.146±0.040	0.085±0.030
MLP (MACCS)	0.696±0.048	0.052±0.018	0.613±0.077	0.462±0.048	0.026±0.083	0.174±0.031	0.065±0.027
Chemprop [80]	0.782±0.062	0.148±0.114	0.676±0.026	0.618±0.03	0.298±0.035	0.375±0.067	0.161±0.024
Graphormer [81, 82]	0.729±0.039	0.096±0.070	-	-	-	-	-

8 Conclusion

In virtual screening, practitioners aim to discover novel molecules and filter their chemical libraries using Tanimoto similarity. Despite this common practice, there are no benchmarks that simulate this particular scenario. In molecular optimization, researchers employ predictive models to guide the optimization process in a step-by-step manner. However, it remains unclear whether these models possess the capacity to distinguish minor modifications.

We identified several limitations in current drug discovery benchmarks and proposed a more realistic and practical alternative in the form of the *Lo-Hi* benchmark. By introducing two tasks, Lead Optimization (Lo) and Hit Identification (Hi), which closely resemble real drug discovery scenarios, we created an environment to evaluate machine learning models under more representative conditions. We emphasize the importance of testing models under conditions similar to their intended application.

Furthermore, the paper critically assesses existing benchmarks and related works, highlighting their inadequacies and the need for better evaluation methods. To address these issues, we suggest alternative datasets. To build them, we designed a novel molecular splitter algorithm for the Hi task.

Different models proved to be better suited to different tasks. Our evaluation of both classical and modern ML models revealed Chemprop as the state-of-the-art for the Hi task, and SVM with ECFP4 fingerprints as the state-of-the-art for the Lo task.

The paper’s key contributions include the introduction of the *Lo-Hi* benchmark, a comprehensive analysis of the limitations of modern ML drug discovery benchmarks, a novel molecular splitter algorithm and the evaluation of modern and classic ML algorithms on the proposed benchmark. This work sets the stage for a more accurate and reliable evaluation of machine learning models in the field of drug discovery, ultimately leading to better decision-making and improved outcomes in the search for new therapeutic compounds.

9 Limitations

We have conducted hyperparameter tuning, although performing it thoroughly poses a challenge [83, 84, 85]. Convincing evidence supporting a particular architecture could be garnered from an open online contest with prizes, accompanied by an undisclosed test dataset. We faced numerous technical difficulties in executing and modifying Graphormer (see Appendix H.7). As such, we cannot definitively determine if Graphormer’s failure is a consequence of its architecture or the result of improper dependency pinning by the authors.

Our findings indicate that the Integer Linear Programming solution proves to be significantly more effective than the greedy approach. However, we have not explored different formulations in our study. Therefore, it is possible that more efficient methods for splitting molecular datasets could exist.

We endeavored to encompass a diverse range of ligand-based drug discovery problems (GPCR inhibition, kinase inhibition, cardiotoxicity, solubility) in our benchmark. However, it is infeasible to capture every potential molecular property prediction task. We advise practitioners to use benchmark results to shortlist models, but also to test them against specific objectives.

10 Future work

Our focus was on medium and large datasets, yet many small datasets contain fewer than 100 data-points. It would be beneficial to have smaller datasets similar to [86] but tailored for Hi generalization.

While our emphasis was on ligand-based drug discovery, where the goal is to predict a molecule’s property, there is also structure-based drug discovery. This approach not only involves predicting molecular properties but also incorporates protein information. Hence, it would be advantageous to have structure-based drug discovery datasets that are divided not just by protein (or pockets [87]) similarity but also with Hi generalization across ligands.

A major ongoing challenge in molecular generative models is ensuring synthesizability, meaning that generated molecules can be made in the real world. Hi splits can help test the generalizability of synthesizability models. But, it’s important to remember that Lo/Hi splits assume similar molecules have similar properties. While this holds for physico-chemical attributes, this premise remains to be validated in the context of feasibility measures.

11 Potential Harmful Consequences

One of the primary concerns arises from the ability to design molecules that are unfamiliar to medical chemists and experts in the field. While the novelty of these compounds can be advantageous for pushing the boundaries of current scientific knowledge, it also raises the potential risk of misuse, especially if malicious actors were to use the system to generate harmful or toxic compounds for hostile purposes. Given their unfamiliar nature, these molecules might not immediately raise flags upon review by experts or during synthesis orders at chemical laboratories. This could open the door for the creation and dissemination of harmful compounds.

12 Acknowledgements

This work was funded by Gleb Pobegailo.

References

- [1] Shu-Feng Zhou and Wei-Zhu Zhong. Drug design and discovery: principles and applications, 2017.
- [2] Jing Lin, Diana C Sahakian, SM De Morais, Jinghai J Xu, Robert J Polzer, and Steven M Winter. The role of absorption, distribution, metabolism, excretion and toxicity in drug discovery. *Current topics in medicinal chemistry*, 3(10):1125–1154, 2003.
- [3] Sabina Podlewska and Rafał Kafel. Metstabon—online platform for metabolic stability predictions. *International journal of molecular sciences*, 19(4):1040, 2018.
- [4] Mohsen Sharifi and Taravat Ghafourian. Estimation of biliary excretion of foreign compounds using properties of molecular structure. *The AAPS journal*, 16:65–78, 2014.
- [5] Patrizia Crivori, Gabriele Cruciani, Pierre-Alain Carrupt, and Bernard Testa. Predicting blood-brain barrier permeation from three-dimensional molecular structure. *Journal of medicinal chemistry*, 43(11):2204–2216, 2000.
- [6] Qiang Tang, Fulei Nie, Qi Zhao, and Wei Chen. A merged molecular representation deep learning method for blood–brain barrier permeability prediction. *Briefings in Bioinformatics*, 23(5), 2022.
- [7] Raimund Mannhold and Han Van de Waterbeemd. Substructure and whole molecule approaches for calculating log p. *Journal of Computer-Aided Molecular Design*, 15:337–354, 2001.
- [8] Ashok K Sharma, Gopal N Srivastava, Ankita Roy, and Vineet K Sharma. Toxim: a toxicity prediction tool for small molecules developed using machine learning and chemoinformatics approaches. *Frontiers in pharmacology*, 8:880, 2017.

- [9] Rakesh Kanji, Abhinav Sharma, and Ganesh Bagler. Phenotypic side effects prediction by optimizing correlation with chemical and target profiles of drugs. *Molecular BioSystems*, 11(11):2900–2906, 2015.
- [10] Brian J Bender, Stefan Gahbauer, Andreas Lutten, Jiankun Lyu, Chase M Webb, Reed M Stein, Elissa A Fink, Trent E Balias, Jens Carlsson, John J Irwin, et al. A practical guide to large-scale docking. *Nature protocols*, 16(10):4799–4832, 2021.
- [11] Reed M Stein, Hye Jin Kang, John D McCorvy, Grant C Glatfelter, Anthony J Jones, Tao Che, Samuel Slocum, Xi-Ping Huang, Olena Savych, Yurii S Moroz, et al. Virtual discovery of melatonin receptor ligands to modulate circadian rhythms. *Nature*, 579(7800):609–614, 2020.
- [12] Ralf Mueller, Alice L Rodriguez, Eric S Dawson, Mariusz Butkiewicz, Thuy T Nguyen, Stephen Oleszkiewicz, Annalen Bleckmann, C David Weaver, Craig W Lindsley, P Jeffrey Conn, et al. Identification of metabotropic glutamate receptor subtype 5 potentiators using virtual high-throughput screening. *ACS chemical neuroscience*, 1(4):288–305, 2010.
- [13] Liying Zhang, Denis Fourches, Alexander Sedykh, Hao Zhu, Alexander Golbraikh, Sean Ekins, Julie Clark, Michele C Connelly, Martina Sigal, Dena Hodges, et al. Discovery of novel antimalarial compounds enabled by qsar-based virtual screening. *Journal of chemical information and modeling*, 53(2):475–492, 2013.
- [14] Bruno J Neves, Rafael F Dantas, Mario R Senger, Cleber C Melo-Filho, Walter CG Valente, Ana CM de Almeida, João M Rezende-Neto, Elid FC Lima, Ross Paveley, Nicholas Furnham, et al. Discovery of new anti-schistosomal hits by integration of qsar-based virtual screening and high content screening. *Journal of medicinal chemistry*, 59(15):7075–7088, 2016.
- [15] Georges E Janssens, Xin-Xuan Lin, Lluís Millan-Ariño, Alan Kavšek, Ilke Sen, Renée I Seinstra, Nicholas Stroustrup, Ellen AA Nollen, and Christian G Riedel. Transcriptomics-based screening identifies pharmacological inhibition of hsp90 as a means to defer aging. *Cell Reports*, 27(2):467–480, 2019.
- [16] Jonathan M Stokes, Kevin Yang, Kyle Swanson, Wengong Jin, Andres Cubillos-Ruiz, Nina M Donghia, Craig R MacNair, Shawn French, Lindsey A Carfrae, Zohar Bloom-Ackermann, et al. A deep learning approach to antibiotic discovery. *Cell*, 180(4):688–702, 2020.
- [17] Zhenqin Wu, Bharath Ramsundar, Evan N Feinberg, Joseph Gomes, Caleb Geniesse, Aneesh S Pappu, Karl Leswing, and Vijay Pande. Moleculenet: a benchmark for molecular machine learning. *Chemical science*, 9(2):513–530, 2018.
- [18] Kexin Huang, Tianfan Fu, Wenhao Gao, Yue Zhao, Yusuf Roohani, Jure Leskovec, Connor W Coley, Cao Xiao, Jimeng Sun, and Marinka Zitnik. Therapeutics data commons: Machine learning datasets and tasks for drug discovery and development. *arXiv preprint arXiv:2102.09548*, 2021.
- [19] Arash Keshavarzi Arshadi, Milad Salem, Arash Firouzbakht, and Jiann Shiun Yuan. Moldata, a molecular benchmark for disease and target based machine learning. *Journal of Cheminformatics*, 14(1):1–18, 2022.
- [20] Yuanfeng Ji, Lu Zhang, Jiaxiang Wu, Bingzhe Wu, Long-Kai Huang, Tingyang Xu, Yu Rong, Lanqing Li, Jie Ren, Ding Xue, et al. Drugood: Out-of-distribution (ood) dataset curator and benchmark for ai-aided drug discovery—a focus on affinity prediction problems with noise annotations. *arXiv preprint arXiv:2201.09637*, 2022.
- [21] Shurui Gui, Xiner Li, Limei Wang, and Shuiwang Ji. Good: A graph out-of-distribution benchmark. *arXiv preprint arXiv:2206.08452*, 2022.
- [22] Ziqiao Zhang, Bangyi Zhao, Ailin Xie, Yatao Bian, and Shuigeng Zhou. Activity cliff prediction: Dataset and benchmark. *arXiv preprint arXiv:2302.07541*, 2023.
- [23] Derek van Tilborg, Alisa Alenicheva, and Francesca Grisoni. Exposing the limitations of molecular machine learning with activity cliffs. *Journal of Chemical Information and Modeling*, 62(23):5938–5951, 2022.

- [24] György M Keserű and Gergely M Makara. Hit discovery and hit-to-lead approaches. *Drug discovery today*, 11(15-16):741–748, 2006.
- [25] Asher Mullard. How much do phase iii trials cost? *Nature Reviews. Drug Discovery*, 17(11): 777–777, 2018.
- [26] Linda Martin, Melissa Hutchens, Conrad Hawkins, and Alaina Radnov. How much do clinical trials cost. *Nat Rev Drug Discov*, 16(6):381–382, 2017.
- [27] Jiankun Lyu, Sheng Wang, Trent E Balius, Isha Singh, Anat Levit, Yurii S Moroz, Matthew J O’Meara, Tao Che, Enkhjargal Algaa, Kateryna Tolmachova, et al. Ultra-large library docking for discovering new chemotypes. *Nature*, 566(7743):224–229, 2019.
- [28] Felix Wong, Satotaka Omori, Nina M Donghia, Erica J Zheng, and James J Collins. Discovering small-molecule senolytics with deep neural networks. *Nature Aging*, pages 1–17, 2023.
- [29] Gary Liu, Denise B Catacutan, Khushi Rathod, Kyle Swanson, Wengong Jin, Jody C Mohammed, Anush Chiappino-Pepe, Saad A Syed, Meghan Fragis, Kenneth Rachwalski, et al. Deep learning-guided discovery of an antibiotic targeting *acinetobacter baumannii*. *Nature Chemical Biology*, pages 1–9, 2023.
- [30] RD Brown and YC Martin. An evaluation of structural descriptors and clustering methods for use in diversity selection. *SAR and QSAR in Environmental Research*, 8(1-2):23–39, 1998.
- [31] Bie Verbist, Günter Klambauer, Liesbet Vervoort, Willem Talloen, Ziv Shkedy, Olivier Thas, Andreas Bender, Hinrich WH Göhlmann, Sepp Hochreiter, QSTAR Consortium, et al. Using transcriptomics to guide lead optimization in drug discovery projects: Lessons learned from the qstar project. *Drug discovery today*, 20(5):505–513, 2015.
- [32] George Papadatos, Anthony WJ Cooper, Visakan Kadirkamanathan, Simon JF Macdonald, Iain M McLay, Stephen D Pickett, John M Pritchard, Peter Willett, and Valerie J Gillet. Analysis of neighborhood behavior in lead optimization and array design. *Journal of chemical information and modeling*, 49(2):195–208, 2009.
- [33] Nathan Brown, Marco Fiscato, Marwin HS Segler, and Alain C Vaucher. Guacamol: benchmarking models for de novo molecular design. *Journal of chemical information and modeling*, 59(3):1096–1108, 2019.
- [34] Tianfan Fu, Cao Xiao, Xinhao Li, Lucas M Glass, and Jimeng Sun. Mimosa: Multi-constraint molecule sampling for molecule optimization. In *Proceedings of the AAAI Conference on Artificial Intelligence*, volume 35, pages 125–133, 2021.
- [35] Wengong Jin, Regina Barzilay, and Tommi Jaakkola. Junction tree variational autoencoder for molecular graph generation. In *International conference on machine learning*, pages 2323–2332. PMLR, 2018.
- [36] Maxime Langevin, Hervé Minoux, Maximilien Levesque, and Marc Bianciotto. Scaffold-constrained molecular generation. *Journal of Chemical Information and Modeling*, 60(12): 5637–5646, 2020.
- [37] William J Godinez, Eric J Ma, Alexander T Chao, Luying Pei, Peter Skewes-Cox, Stephen M Canham, Jeremy L Jenkins, Joseph M Young, Eric J Martin, and W Armand Guiguemde. Design of potent antimalarials with generative chemistry. *Nature Machine Intelligence*, 4(2):180–186, 2022.
- [38] Wenhao Gao, Tianfan Fu, Jimeng Sun, and Connor Coley. Sample efficiency matters: a benchmark for practical molecular optimization. *Advances in Neural Information Processing Systems*, 35:21342–21357, 2022.
- [39] David E Patterson, Richard D Cramer, Allan M Ferguson, Robert D Clark, and Laurence E Weinberger. Neighborhood behavior: a useful concept for validation of “molecular diversity” descriptors. *Journal of medicinal chemistry*, 39(16):3049–3059, 1996.

- [40] Yvonne C Martin, James L Kofron, and Linda M Traphagen. Do structurally similar molecules have similar biological activity? *Journal of medicinal chemistry*, 45(19):4350–4358, 2002.
- [41] Gerald Maggiora, Martin Vogt, Dagmar Stumpfe, and Jurgen Bajorath. Molecular similarity in medicinal chemistry: miniperspective. *Journal of medicinal chemistry*, 57(8):3186–3204, 2014.
- [42] Alex Zhavoronkov and Alán Aspuru-Guzik. Reply to ‘assessing the impact of generative ai on medicinal chemistry’. *Nature Biotechnology*, 38(2):146–146, 2020.
- [43] Pedro Franco, Nuria Porta, John D Holliday, and Peter Willett. The use of 2d fingerprint methods to support the assessment of structural similarity in orphan drug legislation. *Journal of cheminformatics*, 6:1–10, 2014.
- [44] David Rogers and Mathew Hahn. Extended-connectivity fingerprints. *Journal of chemical information and modeling*, 50(5):742–754, 2010.
- [45] John D Holliday, Naomie Salim, Martin Whittle, and Peter Willett. Analysis and display of the size dependence of chemical similarity coefficients. *Journal of chemical information and computer sciences*, 43(3):819–828, 2003.
- [46] Wei Lu, Qifeng Wu, Jixian Zhang, Jiahua Rao, Chengtao Li, and Shuangjia Zheng. Tankbind: Trigonometry-aware neural networks for drug-protein binding structure prediction. *bioRxiv*, pages 2022–06, 2022.
- [47] Seul Lee, Jaehyeong Jo, and Sung Ju Hwang. Exploring chemical space with score-based out-of-distribution generation. In *International Conference on Machine Learning*, pages 18872–18892. PMLR, 2023.
- [48] Hyeoncheol Cho and Insung S Choi. Enhanced deep-learning prediction of molecular properties via augmentation of bond topology. *ChemMedChem*, 14(17):1604–1609, 2019.
- [49] Yoonho Jeong, Jihoo Kim, Yeji Kim, and Insung S Choi. Development of a chemically intuitive filter for chemical graph convolutional network. *Bulletin of the Korean Chemical Society*, 43(7): 934–936, 2022.
- [50] Benson Chen, Regina Barzilay, and Tommi Jaakkola. Path-augmented graph transformer network. *arXiv preprint arXiv:1905.12712*, 2019.
- [51] Prateeth Nayak, Andrew Silberfarb, Ran Chen, Tulay Muezzinoglu, and John Byrnes. Transformer based molecule encoding for property prediction. *arXiv preprint arXiv:2011.03518*, 2020.
- [52] Ross Irwin, Spyridon Dimitriadis, Jiazhen He, and Esben Jannik Bjerrum. Chemformer: a pre-trained transformer for computational chemistry. *Machine Learning: Science and Technology*, 3(1):015022, 2022.
- [53] Yao Zhang et al. Bayesian semi-supervised learning for uncertainty-calibrated prediction of molecular properties and active learning. *Chemical science*, 10(35):8154–8163, 2019.
- [54] Guy W Bemis and Mark A Murcko. The properties of known drugs. 1. molecular frameworks. *Journal of medicinal chemistry*, 39(15):2887–2893, 1996.
- [55] Bihter Das, Mucahit Kutsal, and Resul Das. Effective prediction of drug–target interaction on hiv using deep graph neural networks. *Chemometrics and Intelligent Laboratory Systems*, 230: 104676, 2022.
- [56] Garrett B Goh, Charles M Siegel, Abhinav Vishnu, and Nathan O Hodas. Chemnet: A transferable and generalizable deep neural network for small-molecule property prediction. Technical report, Pacific Northwest National Lab.(PNNL), Richland, WA (United States), 2017.
- [57] Shion Honda, Shoi Shi, and Hiroki R Ueda. Smiles transformer: Pre-trained molecular fingerprint for low data drug discovery. *arXiv preprint arXiv:1911.04738*, 2019.

- [58] Chao Shang, Qinqing Liu, Ko-Shin Chen, Jiangwen Sun, Jin Lu, Jinfeng Yi, and Jinbo Bi. Edge attention-based multi-relational graph convolutional networks. *arXiv preprint arXiv: 1802.04944*, 2018.
- [59] Karim Abbasi, Antti Poso, Jahanbakhsh Ghasemi, Massoud Amanlou, and Ali Masoudi-Nejad. Deep transferable compound representation across domains and tasks for low data drug discovery. *Journal of chemical information and modeling*, 59(11):4528–4539, 2019.
- [60] Prudencio Tossou, Cas Wognum, Michael Craig, Hadrien Mary, and Emmanuel Noutahi. Real-world molecular out-of-distribution: Specification and investigation. 2023.
- [61] Dilyana Dimova and Jürgen Bajorath. Advances in activity cliff research. *Molecular informatics*, 35(5):181–191, 2016.
- [62] Denis Cornaz, Fabio Furini, Mathieu Lacroix, Enrico Malaguti, A Ridha Mahjoub, and Sébastien Martin. Mathematical formulations for the balanced vertex k -separator problem. In *2014 International Conference on Control, Decision and Information Technologies (CoDIT)*, pages 176–181. IEEE, 2014.
- [63] Egon Balas and Cid C de Souza. The vertex separator problem: a polyhedral investigation. *Mathematical Programming*, 103(3):583–608, 2005.
- [64] Stephan Schwartz. An overview of graph covering and partitioning. *Discrete Mathematics*, 345(8):112884, 2022.
- [65] Denis Cornaz, Fabio Furini, Mathieu Lacroix, Enrico Malaguti, A Ridha Mahjoub, and Sébastien Martin. The vertex k -cut problem. *Discrete Optimization*, 31:8–28, 2019.
- [66] Paolo Paronuzzi. Models and algorithms for decomposition problems. 2020.
- [67] Fabio Furini, Ivana Ljubić, Enrico Malaguti, and Paolo Paronuzzi. On integer and bilevel formulations for the k -vertex cut problem. *Mathematical Programming Computation*, 12: 133–164, 2020.
- [68] Yangming Zhou, Gezi Wang, and MengChu Zhou. Detecting k -vertex cuts in sparse networks via a fast local search approach. *IEEE Transactions on Computational Social Systems*, 2023.
- [69] Darko Butina. Unsupervised data base clustering based on daylight’s fingerprint and tanimoto similarity: A fast and automated way to cluster small and large data sets. *Journal of Chemical Information and Computer Sciences*, 39(4):747–750, 1999.
- [70] Yutong Xie, Ziqiao Xu, Jiaqi Ma, and Qiaozhu Mei. How much space has been explored? measuring the chemical space covered by databases and machine-generated molecules. In *The Eleventh International Conference on Learning Representations*.
- [71] Thelma Beatriz González-Castro, Yazmin Hernandez-Diaz, Isela Esther Juárez-Rojop, María Lilia López-Narváez, Carlos Alfonso Tovilla-Zárate, Alma Genis-Mendoza, and Mariela Alpuin-Reyes. The role of c957t, taqi and ser311cys polymorphisms of the drd2 gene in schizophrenia: systematic review and meta-analysis. *Behavioral and Brain Functions*, 12(1): 1–14, 2016.
- [72] Ritushree Kukreti, Sudipta Tripathi, Pallav Bhatnagar, Simone Gupta, Chitra Chauhan, Shobhana Kubendran, YC Janardhan Reddy, Sanjeev Jain, and Samir K Brahmachari. Association of drd2 gene variant with schizophrenia. *Neuroscience letters*, 392(1-2):68–71, 2006.
- [73] V McGuire, SK Van Den Eeden, CM Tanner, F Kamel, DM Umbach, K Marder, R Mayeux, B Ritz, GW Ross, H Petrovitch, et al. Association of drd2 and drd3 polymorphisms with parkinson’s disease in a multiethnic consortium. *Journal of the neurological sciences*, 307(1-2): 22–29, 2011.
- [74] Dongjun Dai, Yunliang Wang, Lingyan Wang, Jinfeng Li, Qingqing Ma, Jianmin Tao, Xingyu Zhou, Hanlin Zhou, Yi Jiang, Guanghui Pan, et al. Polymorphisms of drd2 and drd3 genes and parkinson’s disease: A meta-analysis. *Biomedical reports*, 2(2):275–281, 2014.

- [75] David Mendez, Anna Gaulton, A Patrícia Bento, Jon Chambers, Marleen De Veij, Eloy Félix, María Paula Magariños, Juan F Mosquera, Prudence Mutowo, Michał Nowotka, et al. ChEMBL: towards direct deposition of bioassay data. *Nucleic acids research*, 47(D1):D930–D940, 2019.
- [76] Siddharth J Modi and Vithal M Kulkarni. Vascular endothelial growth factor receptor (vegfr-2)/kdr inhibitors: medicinal chemistry perspective. *Medicine in Drug Discovery*, 2:100009, 2019.
- [77] Cheng Fang, Ye Wang, Richard Grater, Sudarshan Kapadnis, Cheryl Black, Patrick Trapa, and Simone Sciabola. Prospective validation of machine learning algorithms for absorption, distribution, metabolism, and excretion prediction: An industrial perspective. *Journal of Chemical Information and Modeling*, 2023.
- [78] Takaya Saito and Marc Rehmsmeier. The precision-recall plot is more informative than the roc plot when evaluating binary classifiers on imbalanced datasets. *PloS one*, 10(3):e0118432, 2015.
- [79] Kelly Rae Chi. Revolution dawning in cardiotoxicity testing. *Nature reviews. Drug discovery*, 12(8):565, 2013.
- [80] Kevin Yang, Kyle Swanson, Wengong Jin, Connor Coley, Philipp Eiden, Hua Gao, Angel Guzman-Perez, Timothy Hopper, Brian Kelley, Miriam Mathea, et al. Analyzing learned molecular representations for property prediction. *Journal of chemical information and modeling*, 59(8):3370–3388, 2019.
- [81] Yu Shi, Shuxin Zheng, Guolin Ke, Yifei Shen, Jiacheng You, Jiyan He, Shengjie Luo, Chang Liu, Di He, and Tie-Yan Liu. Benchmarking graphormer on large-scale molecular modeling datasets. *arXiv preprint arXiv:2203.04810*, 2022. URL <https://arxiv.org/abs/2203.04810>.
- [82] Chengxuan Ying, Tianle Cai, Shengjie Luo, Shuxin Zheng, Guolin Ke, Di He, Yanming Shen, and Tie-Yan Liu. Do transformers really perform badly for graph representation? In *Thirty-Fifth Conference on Neural Information Processing Systems*, 2021. URL <https://openreview.net/forum?id=0eWoo0xFwDa>.
- [83] Joelle Pineau, Philippe Vincent-Lamarre, Koustuv Sinha, Vincent Larivière, Alina Beygelzimer, Florence d’Alché Buc, Emily Fox, and Hugo Larochelle. Improving reproducibility in machine learning research (a report from the neurips 2019 reproducibility program). *The Journal of Machine Learning Research*, 22(1):7459–7478, 2021.
- [84] Mario Lucic, Karol Kurach, Marcin Michalski, Sylvain Gelly, and Olivier Bousquet. Are gans created equal? a large-scale study. *Advances in neural information processing systems*, 31, 2018.
- [85] Gábor Melis, Chris Dyer, and Phil Blunsom. On the state of the art of evaluation in neural language models. *arXiv preprint arXiv:1707.05589*, 2017.
- [86] Megan Stanley, John F Bronskill, Krzysztof Maziarczyk, Hubert Misztela, Jessica Lanini, Marwin Segler, Nadine Schneider, and Marc Brockschmidt. Fs-mol: A few-shot learning dataset of molecules. In *Thirty-fifth Conference on Neural Information Processing Systems Datasets and Benchmarks Track (Round 2)*, 2021.
- [87] Zaixi Zhang and Qi Liu. Learning subpocket prototypes for generalizable structure-based drug design. *arXiv preprint arXiv:2305.13997*, 2023.
- [88] Tuomo Kallioikoski, Christian Kramer, Anna Vulpetti, and Peter Gedeck. Comparability of mixed ic50 data—a statistical analysis. *PloS one*, 8(4):e61007, 2013.
- [89] Christian Kramer, Tuomo Kallioikoski, Peter Gedeck, and Anna Vulpetti. The experimental uncertainty of heterogeneous public k i data. *Journal of medicinal chemistry*, 55(11):5165–5173, 2012.

A *Lo-Hi* benchmark

Lo-Hi is a practical ML drug discovery benchmark³, comprising two tasks: Hit Identification (Hi) and Lead Optimization (Lo). Hi corresponds to a binary classification problem, wherein the goal is to identify novel hits that differ significantly from the training dataset [10, 11, 16, 27, 28]. This is why there are no molecules in the test set with ECFP4 Tanimoto similarity exceeding 0.4 to the training set. Models are compared using the PR AUC metric.

Lo is a ranking problem that pertains to optimizing molecules or guiding molecular generative models. The test set consists of clusters of similar molecules that are largely dissimilar from the training set, except for one molecule representing a known hit. The task involves ranking the activity of the molecules within clusters, hence we use mean intercluster Spearman correlation to evaluate models. To ensure that the variation in intracluster activity stems from actual differences in activity rather than random noise, we selected clusters demonstrating high variation, as detailed in Appendix B and C.

The datasets each consist of three folds. We advise using the first fold for hyperparameter selection, and then applying these hyperparameters across all folds.

Datasets are released under the MIT license. Authors bear all responsibility in case of violation of rights. Datasets are small .csv files, that is why we are going to keep them in the public GitHub repository. Reviewers can find datasets in data folder.

In this section, we provide further information regarding the datasets and preprocessing steps. The size and diversity of the original datasets are displayed in Table 3.

Table 3: Original datasets

Dataset	Size	#Circles [70] (0.5)	Active fraction
DRD2 (Ki)	8482	837	0.731
HIV	41127	19222	0.035
KDR (IC50)	8826	791	0.643
Sol	2173	1763	0.216
KCNH2 (IC50)	11159	2128	NA

A.1 Data preprocessing

We began by canonicalizing all SMILES using RDKit 2022.9.5.

For DRD2-Hi, DRD2-Lo, KDR-Hi, KDR-Lo and KCNH2-Lo we utilized data from the ChEMBL30 [75] database. We collected data points that measured Ki (for DRD2) and IC50 (for KCNH2 and KDR) with `confidence_score` ≥ 6 . We selected those for which `standard_units` were in "nM". We converted `standard_value` to logarithmic scale, also known as pChEMBL(<https://chembl.gitbook.io/chembl-interface-documentation/frequently-asked-questions/chembl-data-questions#what-is-pchembl>).

For binary DRD2-Hi and KDR-Hi we binarized the data such that log activity values greater than 6 (which is < 10 μ M) were designated as 1, and all others as 0. We removed any ambiguous data points (e.g. with `standard_relation` of "<" and an activity value more than 10 μ M, because those could not be binarized reliably). Following this, we selected data points with identical SMILES, discarding any with differing binarized activities.

For the continuous DRD2-Lo, KDR-Lo and KCNH2-Lo datasets, we selected data points that had `standard_relation` of '=' and a log activity value greater than 5 but less than 9. We selected data points with identical SMILES, discarding any with activity differences greater than 1.0. For the remaining data, we took the median of each group.

³Lo-Hi benchmark: https://github.com/SteshinSS/lohi_neurips2023

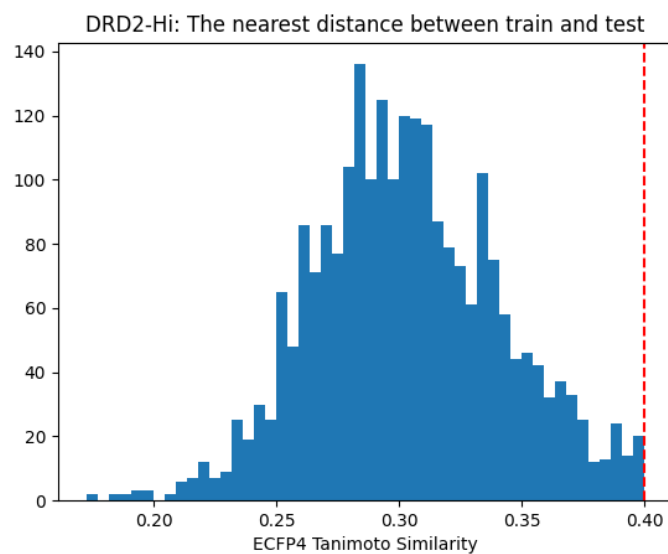


Figure 4: DRD2-Hi: Fold 1

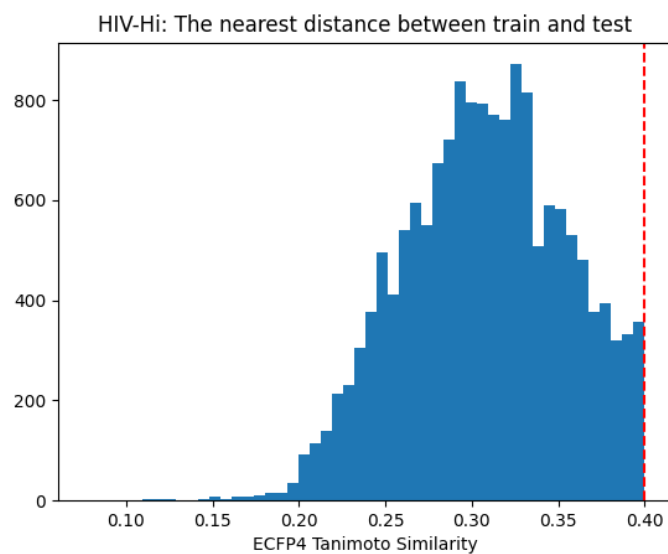


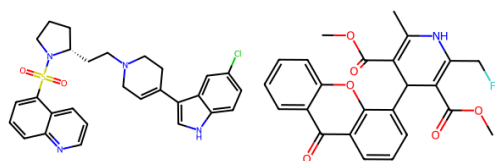
Figure 5: HIV-Hi: Fold 1

Table 4: Hi folds

Dataset	Train 1	Test 1	Train 2	Test 2	Train 3	Test 3
DRD2-Hi	2385	1190	2381	1194	2384	1191
HIV-Hi	15696	7847	15695	7848	15695	7848
KDR-Hi	500	3116	500	3125	500	2285
So1-Hi	1442	721	1442	721	1442	721

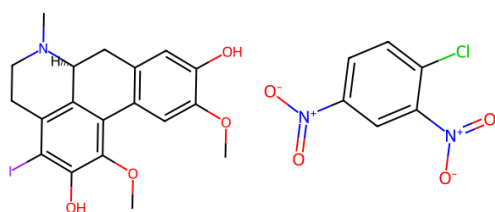
Table 5: Lo folds

Dataset	Train 1	Test 1	Train 2	Test 2	Train 3	Test 3
DRD2-Lo	2206	267	2128	267	2257	262
KCNH2-Lo	3313	406	3313	406	3313	406
KDR-Lo	500	437	500	520	500	417



DRD2-Hi: Fold 1 train

HIV-Hi: Fold 1 train



DRD2-Hi: Fold 1 test

HIV-Hi: Fold 1 test

Figure 6: The most similar pairs of molecules between train and test.

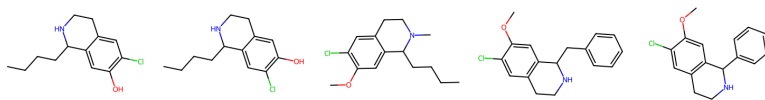


Figure 7: Example of Lo cluster in DRD2-Lo

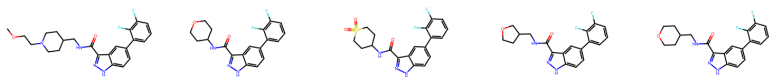


Figure 8: Example of Lo cluster in KCN2-Lo

B Lo dataset is not just noise

Experimental data inherently contain noise. Consequently, selecting similar molecules may result in clusters that possess such a small variation that it could be solely attributable to experimental noise, thereby invalidating the Lo task. This potential issue underlines the importance of ascertaining that the clusters exhibit a significant signal to ensure the validity of the task.

As reported [88], the standard deviation for the same ligand-protein pair’s pIC_{50} is $\sigma_{pIC_{50}} \approx 0.20$ when measured in the same laboratory, and $\sigma_{pIC_{50}} \approx 0.68$ in the ChEMBL database. In similar work [89] standard deviation for ChEMBL pK_i was found to be $\sigma_{pK_i} \approx 0.56$. Therefore, based on these findings, we opted to select only those clusters that displayed a standard deviation exceeding 0.70 for pIC_{50} and more than 0.60 for pK_i . These selection criteria enhance the confidence in the validity of the Lo task by prioritizing clusters with significant intracenter variation.

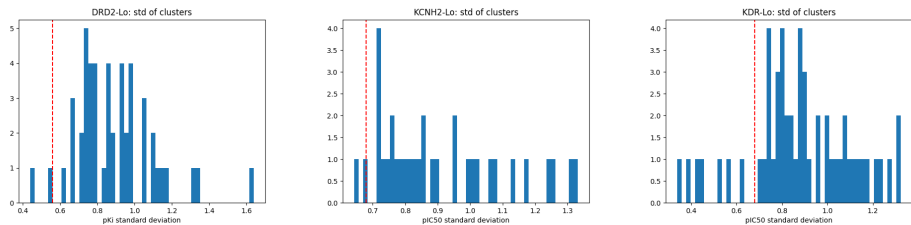


Figure 9: Within cluster variability is higher than noise standard deviation.

C Lo algorithm

The Python implementation can be found in `code/splits.py`.

Algorithm 1 Get Lo Split

Input: List of molecular SMILES S , similarity threshold t , minimum cluster size m , maximum number of clusters M , activity values V , standard deviation threshold std_t

Output: List of SMILES clusters C , list of remaining training SMILES $train_S$

```
1: procedure GETLOSPPLIT( $S, t, m, M, V, std_t$ )
2:    $C, train\_S \leftarrow \text{SELECTDISTINCTCLUSTERS}(S, t, m, M, V, std_t)$ 
3:   for each  $cluster$  in  $C$  do
4:     Move central molecule from  $cluster$  to  $train\_S$ 
5:   end for
6:   return  $C, train\_S$ 
7: end procedure
```

Algorithm 2 Select Distinct Clusters

Input: List of molecular SMILES S , similarity threshold t , minimum cluster size m , maximum number of clusters M , activity values V , standard deviation threshold std_t

Output: List of SMILES clusters C , list of the rest training SMILES $train_S$

```
1: function SELECTDISTINCTCLUSTERS( $S, t, m, M, V, std_t$ )
2:    $train\_S \leftarrow S$ 
3:   Initialize list  $C$  as empty
4:   while length of  $C < M$  do
5:     Compute fingerprints  $F$  from SMILES in  $train\_S$ 
6:     Compute total number of neighbors  $N$  for each fingerprint in  $F$ 
7:     Compute  $STD$  standard deviation of  $V$  of neighbors for each fingerprint in  $F$ 
8:     Set  $central\_idx$  to None
9:     Set  $least\_neighbors$  to  $\max(N)$ 
10:    for each  $idx$  in  $0..|train\_S|$  do ▷ Find the smallest cluster that meets criteria
11:      if  $N[idx] > m$  and  $STD[idx] > std_t$  and  $N[idx] < least\_neighbors$  then
12:         $central\_idx \leftarrow idx$ 
13:         $least\_neighbors \leftarrow N[idx]$ 
14:      end if
15:    end for
16:    if  $central\_idx$  is None then ▷ Exit if there are no more clusters that meet criteria
17:      break
18:    end if
19:    Add  $central\_idx$  molecule and its neighbors to list of clusters  $C$ 
20:    Remove the cluster and its neighbors from  $train\_S$ 
21:  end while
22:  return  $C, train\_S$ 
23: end function
```

D Additional benchmarks analysis

Distribution of Tanimoto Similarity between the nearest molecules between train and test.

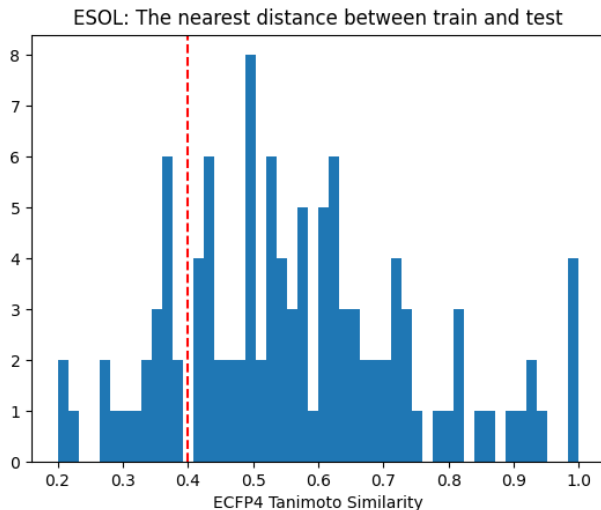


Figure 10: ESOL

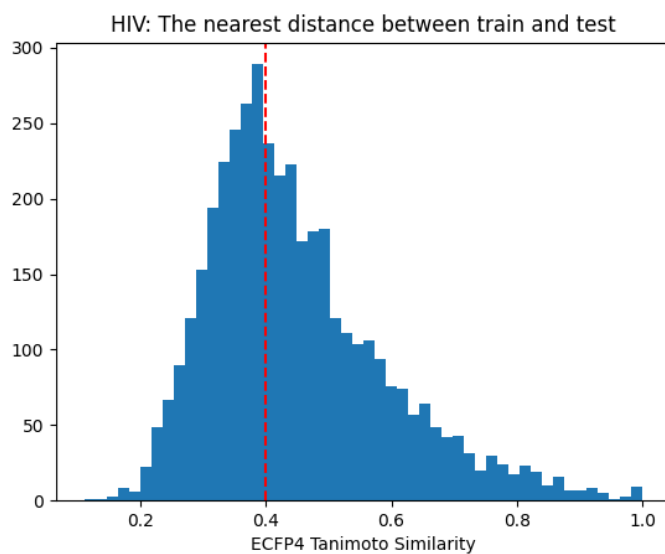


Figure 11: HIV

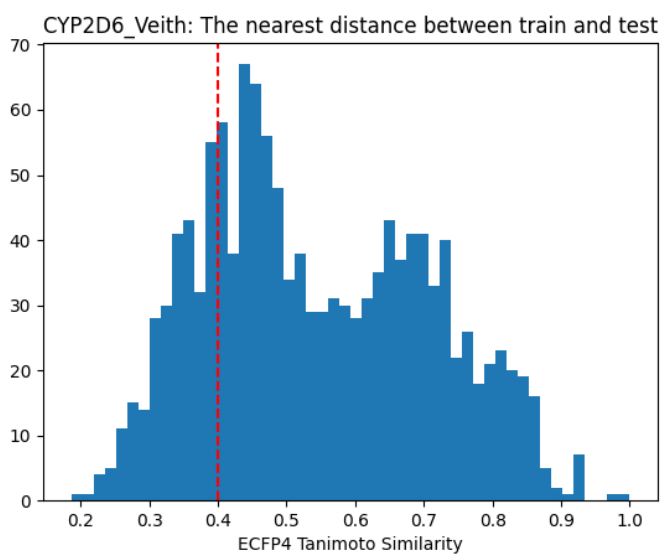


Figure 12: TDC

We additionally analyzed other ligand-based MoleculeNet datasets.

Table 6: Fraction of test molecules in various MoleculeNet datasets with a Tanimoto similarity >0.4 to the train set using ECFP4 fingerprints.

Dataset	Fraction of Test Molecules Similar to Train Set
QM7	0.93
QM8	0.98
QM9	0.99
FreeSolv	0.8
Lipophilicity	0.67
PCBA	>0.93
MUV	0.96
BACE	0.77
Tox21	0.52
SIDER	0.48

E Graph coarsening algorithm

The Python implementation can be found in `code/min_vertex_k_cut.py`. We are planning to release it as a pip package.

Algorithm 3 Calculate Neighbors

Input: Graph $G = (V, E)$, similarity threshold θ

Output: List of tuples $n_neighbors$

```

1: function CALCULATENEIGHBORS( $G, \theta$ )
2:   Initialize list  $n\_neighbors$  as empty
3:   for each node  $v$  in  $V$  do
4:     Initialize  $total\_neighbors$  as 0
5:     for each edge  $e$  incident on node  $v$  do
6:       if  $e['similarity'] > \theta$  then
7:          $total\_neighbors \leftarrow total\_neighbors + 1$ 
8:       end if
9:     end for
10:    Append ( $total\_neighbors$ , index of  $v$ ) to  $n\_neighbors$ 
11:  end for
12:  return  $n\_neighbors$ 
13: end function

```

Algorithm 4 Cluster Nodes

Input: Sorted list $n_neighbors$, Graph $G = (V, E)$, similarity threshold θ

Output: Cluster assignment $node_to_cluster$, number of clusters $total_clusters$

```
1: function CLUSTERNODES( $n\_neighbors, G, \theta$ )
2:   Initialize array  $node\_to\_cluster$  of size  $|V|$  as  $-1$ 
3:   Initialize  $total\_clusters$  as 1
4:   for each tuple  $(count, node)$  in  $n\_neighbors$  do
5:     if  $node\_to\_cluster[node] = -1$  then
6:        $node\_to\_cluster[node] \leftarrow total\_clusters$  ▷ Assign new cluster
7:       for each edge  $e$  incident on node  $node$  do
8:         if  $e[‘similarity’] > \theta$  then
9:            $adjacent\_node \leftarrow e[1]$ 
10:          if  $node\_to\_cluster[adjacent\_node] = -1$  then
11:             $node\_to\_cluster[adjacent\_node] \leftarrow total\_clusters$ 
12:          end if
13:        end if
14:      end for
15:       $total\_clusters \leftarrow total\_clusters + 1$ 
16:    end if
17:  end for
18:  return  $node\_to\_cluster, total\_clusters$ 
19: end function
```

Algorithm 5 Build Coarse Graph

Input: Cluster assignment $node_to_cluster$, number of clusters $total_clusters$, Graph $G = (V, E)$

Output: Coarsened Graph G_{coarse}

```
1: function BUILDCOARSEGRAPH( $node\_to\_cluster, total\_clusters, G$ )
2:   Compute  $clusters\_size$ , count of each unique element in  $node\_to\_cluster$ 
3:   Initialize  $G_{coarse}$  as an empty graph
4:   for  $cluster$  in 0 to  $total\_clusters - 1$  do ▷ Add nodes
5:     Add node  $cluster$  with weight  $clusters\_size[cluster]$  to  $G_{coarse}$ 
6:   end for
7:   for  $cluster$  in 0 to  $total\_clusters - 1$  do ▷ Add edges
8:     Initialize  $connected\_clusters$  as an empty set
9:     Get nodes of  $cluster$  as  $this\_cluster\_indices$  where  $node\_to\_cluster$  equals  $cluster$ 
10:    for each  $node$  in  $this\_cluster\_indices$  do
11:      for each edge  $e$  incident on node  $node$  do
12:        Add  $node\_to\_cluster[e[1]]$  to  $connected\_clusters$ 
13:      end for
14:    end for
15:    for each  $connected\_cluster$  in  $connected\_clusters$  do
16:      Add edge from  $cluster$  to  $connected\_cluster$  in  $G_{coarse}$ 
17:    end for
18:  end for
19:  return  $G_{coarse}$ 
20: end function
```

Algorithm 6 Main Procedure

Input: Graph $G = (V, E)$, similarity threshold θ

Output: Coarsened graph G_{coarse}

```
1: procedure COARSEGRAPH( $G, \theta$ )
2:    $n\_neighbors \leftarrow \text{CALCULATENEIGHBORS}(G, \theta)$ 
3:   Sort  $n\_neighbors$  in descending order of first element of each tuple
4:    $node\_to\_cluster, total\_clusters \leftarrow \text{CLUSTERNODES}(n\_neighbors, G, \theta)$ 
5:    $G_{coarse} \leftarrow \text{BUILDCOARSEGRAPH}(node\_to\_cluster, total\_clusters, G)$ 
6:   return  $G_{coarse}$ 
7: end procedure
```

F Hi-split predicts virtual screening hit rate better than scaffold split

For effective virtual screening, predicting experimental outcomes prior to experimentation is paramount. In this study, we compare the predictive performance of the novel Hi-split approach with the traditional scaffold split method under a Hit Identification scenario. Following existing literature [10, 11, 16, 27, 28], we simulate testing on novel molecules with an ECFP4 Tanimoto similarity of ≤ 0.4 to the training set. The dataset is partitioned using both splitting methods to form separate training and validation sets for hyperparameter selection. Hyperparameter search is performed for gradient boosting on ECFP4 fingerprints, identified as the most efficient Hi model that facilitates quick training.

After selecting the optimal hyperparameters, performance metrics are computed on the validation set. Subsequently, the model is retrained on the combined training and validation sets, and performance metrics for the hold-out test set are calculated to simulate the application of a trained model in virtual screening. The results are summarized in Table 7.

Table 7: Hi-split vs scaffold split

Dataset	Validation	Test
DRD2-Hi (Hi split)	0.603	0.677
DRD2-Hi (Scaffold split)	0.872	0.663
HIV-Hi (Hi split)	0.069	0.084
HIV-Hi (Scaffold split)	0.189	0.078

The Hi-split method demonstrates superior predictive performance for virtual screening hit rate compared to the scaffold split method, which is over-optimistic in the Hit Identification scenario. It also improved the test evaluation metric, although the difference is not substantial. The improved performance of the Hi-split may be attributed to the selection of more regularized models.

G Novelty consensus analysis

We have reproduced the work presented in [43] using binary ECFP4 fingerprints, as calculated by RDKit version 2022.9.5. The results can be found in Figure 13. For this particular work, we selected 0.40 as the novelty threshold.

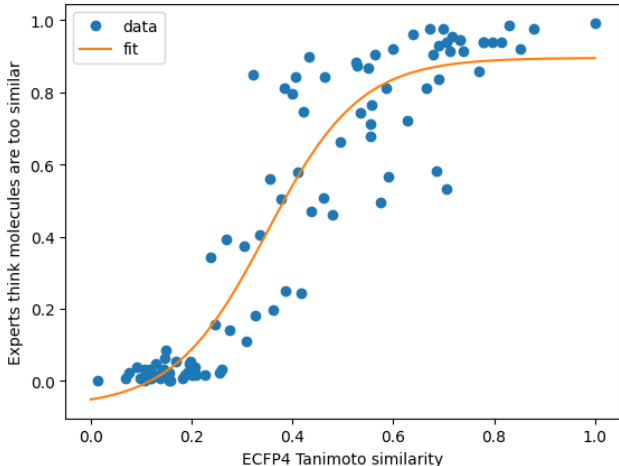


Figure 13: Sigmoid fit to [43] data

H Hyperparameter optimization

We used random or grid search to optimize hyperparameters for all models except for the Graphormer, which was too slow for meticulous hyperparameter search. Here we provide optimization parameters and additional commentary on the training.

We utilized a single NVIDIA RTX 2070 SUPER with CUDA 11.7 and calculated binary 1024 ECFP4 and MACCS fingerprints using RDKit 2022.9.5.

H.1 Dummy baseline

Always predicts the same constant value.

H.2 KNN

We used `scipy.spatial.distance.jaccard` as the distance metric, as it outperformed the standard Euclidian distance in our use case. We used grid search with all combinations of parameters. For ECFP4 it was:

```
params = {
    'n_neighbors': [3, 5, 7, 10],
    'weights': ['uniform', 'distance'],
}
```

and for MACCS:

```
params = {
    'n_neighbors': [3, 5, 7, 10, 12, 15],
    'weights': ['uniform', 'distance'],
}
```

H.3 Gradient Boosting

We used 30 iterations of random search with these parameters:

```
params = {
    'n_estimators': [10, 50, 100, 150, 200, 250, 500],
    'learning_rate': [0.01, 0.1, 0.3, 0.5, 0.7, 1.0],
    'subsample': [0.4, 0.7, 0.9, 1.0],
    'min_samples_split': [2, 3, 5, 7],
    'min_samples_leaf': [1, 3, 5],
    'max_depth': [2, 3, 4],
    'max_features': [None, 'sqrt']
}
```

H.4 SVM

We used grid search with these parameters:

```
params = {
    'C': [0.1, 0.5, 1.0, 2.0, 5.0],
}
```

H.5 MLP

We implemented a feed-forward neural network using Pytorch 2.0.0+cu117 and Pytorch Lightning 2.0.2. It consisted of several feed-forward layers with optional dropout layers. We used early stopping to prevent overfitting with patience 20 for the Hi tasks, and 10 for the Lo tasks. We used learning rate 0.01. We used batch size 32. We conducted 30 iterations of random search. For ECFP4 we used these parameters:

```

param_dict = {
    'layers': [
        [1024, 32, 32],
        [1024, 16, 16],
        [1024, 32],
        [1024, 8, 4],
        [1024, 4]
    ],
    'dropout': [0.0, 0.0, 0.2, 0.4, 0.6],
    'l2': [0.0, 0.0, 0.001, 0.005, 0.01],
}

```

For MACCS we used these parameters:

```

param_dict = {
    'layers': [
        [167, 32, 32],
        [167, 16, 16],
        [167, 32],
        [167, 8, 4],
        [167, 4]
    ],
    'dropout': [0.0, 0.0, 0.2, 0.4, 0.6],
    'l2': [0.0, 0.0, 0.001, 0.005, 0.01],
}

```

After the selection of the best hyperparameters, we selected a fixed number of the training epochs using early stopping. We used the same number of epochs for all the folds.

H.6 Chemprop

We used Chemprop 1.5.2 with rdkit features. We found the evaluation metrics to be a little better with them, but it was SOTA for Hi even without them:

```

'--features_generator rdkit_2d_normalized',
'--no_features_scaling',

```

We used 20 iterations of random search with these parameters:

```

param_dict = {
    '--depth': ['3', '4', '5', '6'],
    '--dropout': ['0.0', '0.2', '0.3', '0.5', '0.7'],
    '--ffn_hidden_size': ['600', '1200', '2400', '3600'],
    '--ffn_num_layers': ['1', '2', '3'],
    '--hidden_size': ['600', '1200', '2400', '3600']
}

```

We selected the number of epochs using only the first fold. After the hyperparameters were selected, we trained the model and did not expose it to the test data. The full command for training Chemprop for HIV-Hi dataset:

```

chemprop_train --data_path data/hi/hiv/train_1.csv --dataset_type classification \
--save_dir checkpoints/hi/hiv/ \
--config_path configs/hiv_hi \
--separate_val_path data/hi/hiv/train_1.csv \
--separate_test_path data/hi/hiv/train_1.csv \
--metric 'prc-auc' \
--epochs 40 \
--features_generator rdkit_2d_normalized \
--no_features_scaling

```

For the DRD-Hi the best hyperparameters were:

```
{
  "depth": 6,
  "dropout": 0.0,
  "ffn_hidden_size": 2400,
  "ffn_num_layers": 1,
  "hidden_size": 2400
}
```

For the HIV-Hi the best hyperparameters were:

```
{
  "depth": 6,
  "dropout": 0.2,
  "ffn_hidden_size": 3600,
  "ffn_num_layers": 2,
  "hidden_size": 3600
}
```

H.7 Graphormer

We used Graphormer with the last commit 77f436db46fb9013121289db670d1a763f264153. We applied two fixes, that we found in issues <https://github.com/microsoft/Graphormer/issues/158#issuecomment-1500311589> and <https://github.com/microsoft/Graphormer/issues/130#issuecomment-1207316808> that solved our problems. However, we set up an in-house Graphormer some time ago and currently, it cannot be reinstalled from scratch due to multiple broken dependencies.

We modified code to calculate and track PR AUC metrics, to add our datasets, and to evaluate trained models. We manually optimized the hyperparameters over approximately 10 iterations. We found Graphormer to be inferior to Chemprop, which is consistent with our previous experience with different datasets.

We faced numerous technical difficulties in executing and modifying Graphormer [81, 82] due to improper dependency pinning by the authors. We found the training to be slow, which limited our ability to optimize hyperparameters. Because of technical difficulties, we decided not to test it for the Lo task.

H.8 HIV-Hi balance

HIV-Hi is a highly unbalanced binary classification problem with only 3% of positive examples. Due to this imbalance, we experimented with weighted options of classical ML algorithms and manually resampled positive examples for neural networks.

I Spearman distribution

The test set of the Lo datasets is composed of molecular clusters. To evaluate the models, the Spearman correlation coefficient is calculated within each cluster, comparing the actual activity values to the predicted ones. The final Lo metric is the average of the Spearman coefficients across all clusters.

In the following, we present a histogram of Spearman coefficients for the best models across various datasets. Note that the KDR-Lo dataset is more challenging than both DRD2-Lo and KCNH2-Lo.

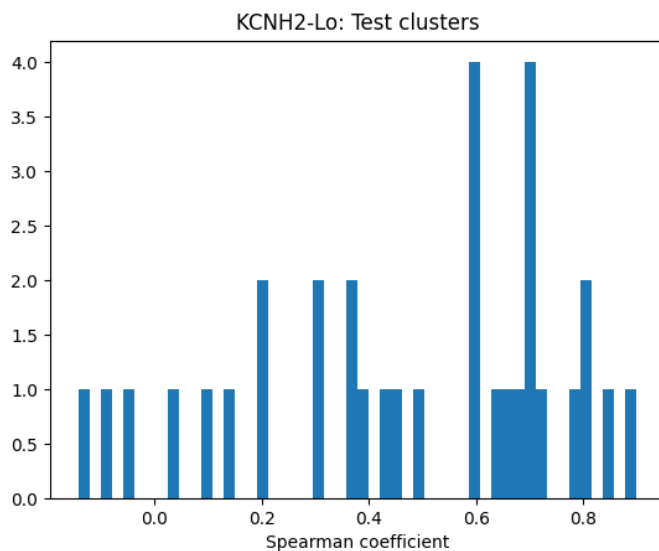


Figure 14: KCNH2-Lo Spearman coefficient distribution for SVM-ECFP4

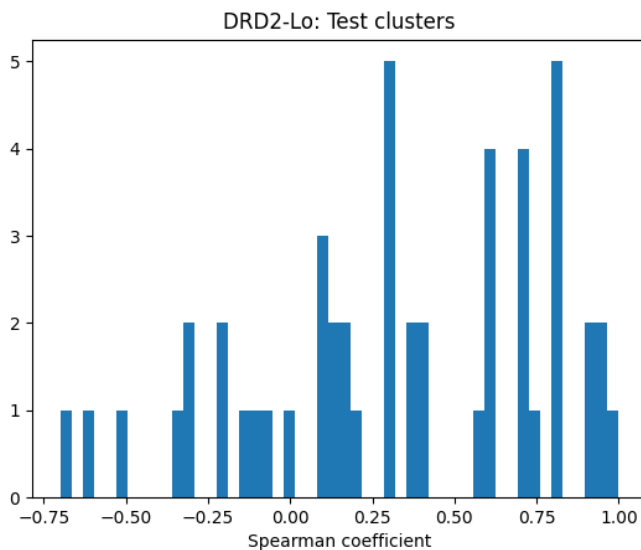


Figure 15: DRD2-Lo Spearman coefficient distribution for SVM-ECFP4

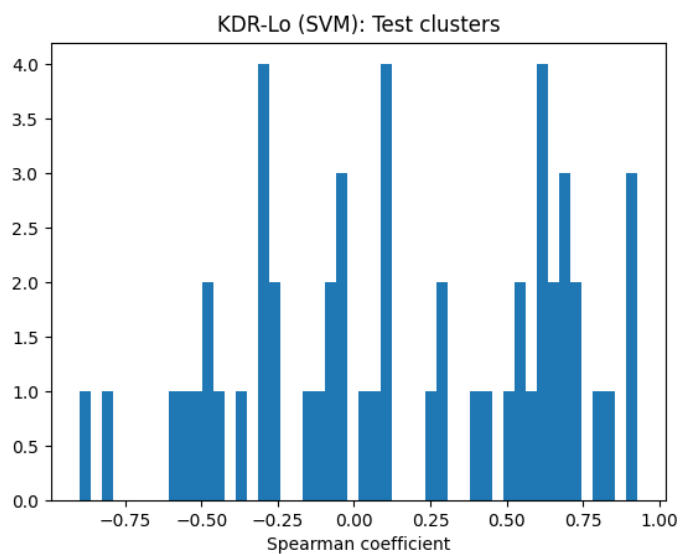


Figure 16: KDR-Lo Spearman coefficient distribution for SVM-ECFP4

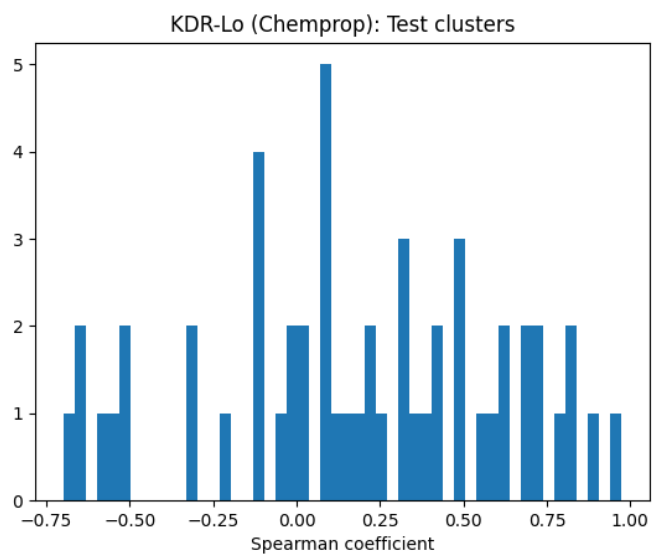


Figure 17: KDR-Lo Spearman coefficient distribution for Chemprop